PCCP

Accepted Manuscript

New Models for Predicting Thermophysical Properties of Ionic Liquid Mixtures

Ying Huang, Xiangping Zhang*, Yongsheng Zhao, Shaojuan Zeng, Haifeng Dong, Suojiang Zhang*

Beijing Key Laboratory of Ionic Liquids Clean Process, State Key Laboratory of Multiphase Complex Systems, Key Laboratory of Green Process and Engineering, Institute of Process Engineering, Chinese Academy of Sciences, Beijing 100190, China

Abstract

Potential applications of ILs require the knowledge of physicochemical properties of ionic liquid (IL) mixtures. In this work, a series of semi-empirical models were developed to predict density, surface tension, heat capacity and thermal conductivity of IL mixtures. Each semi-empirical model only contains one new characteristic parameter, which can be determined using one experimental data. Besides, as another effective tool, artificial neural network (ANN) models were also established. The two kinds of models were verified by a total of 2304 experimental data points of binary mixtures of ILs and molecular compounds. The overall average absolute deviations (AARDs) of both the semi-empirical and ANN models are less than 2%. Compared to the previous reported models, these new semi-empirical models require less adjustable parameters and can be applied in wider application range.

Keywords: IL mixtures; Thermophysical properties; Semi-empirical models; Artificial neural networks

*Corresponding author. Tel./Fax: +86 01062558174
E-mail address: xpzhang@ipe.ac.cn, sjzhang@ipe.ac.cn

1. Introduction

Ionic liquids (ILs) have been increasingly studied both in academy and industry[1, 2] because of their unique properties, such as wide electrochemical window, extremely low vapor pressure, high solvating capacity and thermal stability. Potential applications of ILs require the knowledge of physicochemical properties not only for pure ILs, but also for their mixtures with different solvents. Because there are uncountable combinations of cations, anions and molecular solvents, it is costly and time-consuming to measure all the properties. Therefore, it is necessary to develop available models to predict the properties of IL mixtures[3-5]. The typical predictive equations and correlations for IL mixtures were summarized in Table 1.

Table 1. Summary of the current literature about thermophysical prediction of IL mixtures

Specific model	Property	ΔT (K)	Number of IL mixtures	Predictive deviations	Number of parameters
COSMO–SAC model combined with mixing rules and PR EOS[6]	Density	288-323	3	Deviations<3%	>6
Redlich–Kister polynomial equation[7] $\Delta\sigma_{ij} = x_i x_j \sum_k A_k (x_i - x_j)^k$	Surface tension	283-313	6	Standard deviations <0.1	4
Extended Spencer and Danner equation[8] $\rho_{mix.} = \left(\sum_i \frac{P_{ci}}{R x_i T_{ci}}\right) Z_{RAmix.}^{-(1+\tau_{mix}^{2/7})}$	Density	278-358	14	*AARD* =0.50%	4
Perturbed hard-sphere EOS[9] $\frac{P}{\rho kT} = \frac{1+\eta+\eta^2-\eta^3}{(1-\eta)^3} - \frac{\rho}{kT}\sum_i^m \sum_j^m x_i x_j a(T)_{ij}$	Density	278-353	14	*AARD* =0.38%	>7
Extended Tao and Mason EOS[10] $\frac{P}{\rho kT} = 1 + \rho \sum_{ij} x_i x_j \left((B_2)_{ij} - \alpha_{ij}\right) + \rho \sum_{ij} x_i x_j \alpha_{ij} G_{ij} + \rho \sum_{ij} x_i x_j (I_1)_{ij}$	Density	198-343	13	*AARD* =1.69%	4
Redlich–Kister equation[11] $C_p^E / (J \cdot mol^{-1} \cdot K^{-1}) = x_1 x_2 \sum_{i=1}^n B_i (x_1 - x_2)^{i-1}$	Heat capacity	283.15–343.15	2	*AARD* =0.1%	6

Density of IL mixtures is a fundamental property, and the related predictive models have been reported more frequently[12, 13]. The reported models can be mainly summarized as two categories: 1) empirical correlations such as Redlich–Kister polynomial equation[14-20] and Lorentz–Lorenz equation[21, 22]. These models relied on lots of experimental density data for fitting parameters. 2) equation of state (EOS)-based models, such as Perturbed hard-sphere EOS[8] and SAFT + Cubic EOS[23], which required more sophisticated thermodynamic calculations.

Among the many unique properties, the surface tension plays a special role in process design via affecting the mass and heat transfer at the interface[24, 25]. Many articles have reported the predictive models of surface tension of pure ILs[26-28]. However, the surface tension prediction of IL mixtures was less explored and understood[25]. The current models are all developed on the basis of mixtures of molecular compounds, which can also be divided into two categories: 1) correlations and empirical relations, which are easy to be used but limited to a few compounds. Gardas et al.[29] used a parachor estimation method and a solubility model to correlate the surface tensions of mixtures of imidazolium-based ILs with water or n-alkanes. The parameters in their models were obtained by fitting the experimental interfacial tension data or solubility data. Fu et al.[30] recently correlated the surface tensions of two ternary systems containing ILs using an empirical correlation with 9 adjustable parameters. Although the above empirical models could accurately correlate surface tension, their predictive performance are unknown. 2) Models derived from thermodynamics, which require more experimental data and sophisticated calculations. Xu et al.[31] developed a modified Hildebrand−Scott equation based on UNIFAC model, and the surface tension at 298.15 K was required for the regression of energy parameters. Rilo et al.[32] developed a theoretical equation based on the Bahe–Varela pseudo-lattice model. Recently, Ghasemian Lemraski et al.[33] predicted the surface tensions of IL mixtures based on the CSGC model (corresponding-states group-contribution method), HSEG model (extended Guggenheim's ideal solution model) and parachor model, and the *AARD* were all higher than 5%.

Heat capacity and thermal conductivity are necessary in process design, especially in the calculation of heat duty of equipment. However, the prediction of heat capacity and thermal conductivity of IL mixtures are rarely reported. Most studies focused on correlating the excess molar heat capacity by a Redlich–Kister equation[11, 34, 35] with six adjustable parameters, which required sophisticated fitting procedures for each mixture. Therefore, it is imperative to develop effective models for predicting the thermophysical properties of IL mixtures and avoid difficult calculations to satisfy the demands of engineering.

The other widely accepted prediction method is artificial neural network (ANN), which can be used for different class of materials[36],. ANN represents a complex configuration, including input, hidden, and output layers with many neurons[37, 38], which can transform the data through suitable activation functions thus model the nonlinear behavior of properties. In recent years, the predictive ability of ANN has been tested and applied by several researchers for modeling various properties of pure ILs, such as melting points[39], density[40], viscosity [41, 42], heat capacity [43], thermal conductivity[44] and electric conductivity[43]. Thus it is essential to use the ANN technique to predict the properties of IL mixtures.

We have successfully predicted the thermophysical properties of pure ILs based on corresponding states correlations[3], thus it is convenient and meaningful to develop general models for predicting thermophysical properties of IL mixtures. This work focuses on predicting the density, surface tension, heat capacity and thermal conductivity of IL mixtures using new semi-empirical models and ANN method. Some key characteristic parameters were defined to represent the excess magnitudes of properties. The molecular components of the studied IL mixtures included common solvents: water, alcohols, alkanes, ketones, esters, acid, dimethyl sulfoxide, acetonitrile, and tetrahydrofuran.

2. Methodology

2.1 Database

In this study, comprehensive property of binary mixtures of IL and molecular solvent at different temperatures and compositions were collected from lots of literature, including experimental data of densities of 25 binary mixtures, surface tensions of 28 binary mixtures, heat capacities of 9 binary mixtures and thermal conductivities of 3 binary mixtures, as shown in Tables 1-8. The ILs contain the cations of imidazolium [Im], pyridinium [Py], ammonium [N] and phosphonium [P] and the anions of tetrafluoroborate [BF_4], hexafluorophosphate [PF_6], bis(trifluoromethylsulfonyl)imide [BTI], bromide [Br], alkyl sulfate [RSO_4], dimethyl phosphate [DMP], trifluoromethylsulfonate [TfO], nitrate [NO_3] and dicyanamide [Dca]. The molecular components intended to cover common solvents such as water, alcohols, dimethyl sulfoxide, acetonitrile, and tetrahydrofuran.

2.2 Semi-empirical models

According to the effect of addition of ILs on the densities of molecular compounds, the following semi-empirical relationship was proposed:

$$\rho_m = x_1\rho_1 + x_2\rho_2 + \delta\rho \qquad (1)$$

$$\delta\rho = a x_1 x_2 (\rho_1 + \rho_1) T^{1/2} \qquad (2)$$

where ρ_m is the density of the mixture, x_1 and x_2 are the molar fraction of molecular compounds and ILs, respectively. ρ_1 and ρ_2 are the density of pure molecular compounds and ILs, respectively. $\delta\rho$ denotes the excess magnitudes of density of IL mixtures. a represents the characteristic parameter of density of each IL mixture, which can be determined by only one experimental density data point of the specific IL mixture .

The surface tensions of IL mixtures were calculated by Eq. 3, which was similar to Eq.1. It is obvious that the surface tension behavior of alcohol-based and water-based IL mixtures exhibits opposite trends[25]. Therefore, different models for water-based mixtures and organic-based mixtures were employed, as expressed by Eq.4 and Eq.5, respectively.

$$\sigma_m = x_1\sigma_1 + x_2\sigma_2 + \delta\sigma \qquad (3)$$

$$\delta\sigma = bx_1(\sigma_1 + \sigma_2)T^{1/2} \qquad (4)$$

$$\delta\sigma = b' x_1 x_2(\sigma_1 + \sigma_2)T^{1/2} \qquad (5)$$

where σ_m is the surface tension of the mixture, x_1 and x_2 are the molar fraction of molecular compounds and ILs, respectively. σ_1 and σ_2 are the surface tension of pure molecular compounds and ILs, respectively. The surface tension of pure ILs were taken from literature or estimated by the Brock-Bird equation[45]. $\delta\sigma$ denotes the excess magnitudes of surface tension of IL mixtures. *b* and *b'* denote the characteristic parameter of surface tension of water-based and organic-based IL mixture, respectively, which can be determined on the basis of only one surface tension data of the specific IL mixture.

The heat capacities of IL mixtures were calculated by the following models, which were similar to Eq.1 and Eq.2.

$$C_{pm} = x_1 C_{p1} + x_2 C_{p2} + \delta C_p \qquad (6)$$

$$\delta C_p = c x_1 x_2 (C_{p1} + C_{p2})T^{1/2} \qquad (7)$$

where C_{pm} is the heat capacity of the mixture, x_1 and x_2 are the molar fraction of molecular compounds and ILs, respectively. C_{p1} and C_{p2} are the heat capacity of pure molecular compounds and ILs, respectively. δC_p denotes the excess magnitudes of heat capacity of IL mixtures. *c* represents the characteristic parameter of heat capacity of each IL mixture, which can be determined by only one heat capacity data point of the specific IL mixture.

The thermal conductivity of IL mixtures were calculated by Eq.8 and Eq.9.

$$\lambda_m = w_1\lambda_1 + w_2\lambda_2 + \delta\lambda \qquad (8)$$

$$\delta\lambda = d w_1 w_2(\lambda_1 + \lambda_2)T^{1/2} \qquad (9)$$

where λ_m is the thermal conductivity of the mixture, w_1 and w_2 are the mass fraction of molecular compounds and ILs, respectively. λ_1 and λ_2 are the thermal conductivity of pure molecular compounds and ILs, respectively. $\delta\lambda$ denotes the excess magnitudes of thermal conductivity of IL mixture. *d* represents the characteristic parameter of thermal conductivity of each IL mixture, which can be calculated on the basis of only one thermal conductivity data of the specific IL mixture.

2.3 Artificial neural network models

The structure of ANN models was illustrated in Figure 1, which is a kind of the most common used multilayer perceptron (MLP). The input layer comprised of five variables: temperature, mole fraction of molecular compounds and ILs, thermophysical properties (surface tension, heat capacity and thermal conductivity) of pure molecular compounds and ILs. And the ANN models require no fitted parameters. The number of hidden layers was considered as one, which was able to correlate any type of nonlinear relation[46]. The experimental data of thermophysical properties of IL mixtures were the target of the output layer.

The ANN was trained with Levenberg－Marquardt learning algorithm[47, 48] with high-speed training capabilities. The whole set of available data were randomly divided into three groups for training (70%), validation (15%) and testing (15%) the model.

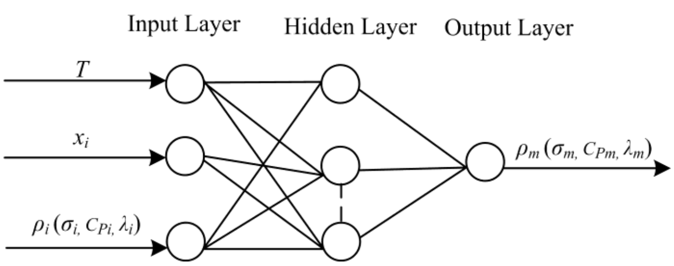

Figure 1. Used MLP structure of ANN

2.4 Statistical assessments

To evaluate the efficiency and accuracy of the proposed semi-empirical models and ANN models, some statistical parameters were utilized, namely, minimum relative deviation

(RD_{min}), maximum relative deviation (RD_{max}), average absolute relative deviation (*AARD*), and coefficient of determination (R^2). The mathematical definitions of the parameters were given as below:

$$RD(\%) = 100 \times (Q_{im}^{cal} / Q_{im}^{\exp} - 1.0) \tag{10}$$

$$AARD(\%) = 100 \times \sum_{i=1}^{N_P} \left| Q_{im}^{cal} / Q_{im}^{\exp} - 1.0 \right| / N_P \tag{11}$$

$$R^2 = \frac{\sum_{i=1}^{N_P} \left(Q_{im}^{\exp} - \bar{Q}_m \right)^2 - \sum_{i=1}^{N_P} \left(Q_{im}^{\exp} - Q_{im}^{cal} \right)^2}{\sum_{i=1}^{N_P} \left(Q_{im}^{\exp} - \bar{Q}_m \right)^2} \tag{12}$$

where Q denotes the studied thermophysical properties, i.e. ρ, σ, C_p and λ. N_p represents the total number of data points of each property, the superscripts *'exp'* and *'cal'* denote the experimental value from literature and calculated value, respectively. $\bar{Q}_m$ is the average value of the experimental property of mixtures.

3. Results and discussion

1104 density data points of 33 binary mixtures, 573 surface tension data points of 28 binary mixtures, 603 heat capacity data points of 9 binary mixtures and 24 thermal conductivity data points of 3 binary mixtures over wide range of temperature and mole fraction were collected to correlate model parameters and verify the semi-empirical models (see Eqs.1-9). Moreover, as another useful technique of property prediction, the ANN models were designed to estimate the above thermophysical properties of IL mixtures. The correlated and predicted results of each data point of all the thermophysical properties are given in the Supplementary materials that form part of this paper.

3.1 Prediction results of Density

Semi-empirical model The 1104 density data points of 33 binary systems were divided into two sets. One was correlation dataset for the determination of the parameter *a*, and the other was validation dataset, which was applied to test the predictive performance of the semi-empirical model for density. As described above, the determination of parameter *a* only required one experimental data point of each system. Thus 33 data points of 33 binary systems were selected as correlation dataset, which was listed in Table 1. The selection principle was that mole fraction of each component was near 0.5 and the temperature was near 298.15K. It can be seen from Table 2 that all the relative deviation of each mixture are less than ±0.1%, which indicates the semi-empirical model for density can achieve highly accurate correlation results.

With the semi-empirical model for density (Eqs.1-2) and correlated parameters (see Table 2), further prediction can be performed. As shown in Figure 2, the predicted results by the semi-empirical model display good agreement with experimental density. Furthermore, the histogram of the relative prediction deviations was given in Figure 3. It can be seen that 81% of the deviations were within ±2%, and only 4.3% were larger than ±5%. Detailed prediction deviations of each binary system were summarized in Table 3, and the overall prediction *AARD* was only 1.1%. It is obvious that [C_6MIm][Cl] +[C_6MIm][PF_6] has the highest prediction accuracy, and the alcohol-based IL mixtures give relatively lower prediction accuracy. This is mainly resulted from the higher discrepancy between ILs and alcohol. The highest deviation was observed in 2-Propanol (1) + [MOA][BTI] (2) at x_1=0.9. This above results implied that the semi-empirical model had relatively poor prediction performance at high concentration of lighter molecular solvents. In general, the semi-empirical model is accurate not only for density correlation of IL mixtures, but also for prediction. Comparing to the published models, the current model can be accurately used for wider range of IL mixtures and diminish the number of adjustable parameter to 1, which is much easier to be obtained.

Table 2. Correlated results of density of 25 IL mixtures using the semi-empirical model (Eqs.1-2)

Parameter *a*	Binary system	x_1	*T*/ K	ρ_m^{exp} /(g cm^{-3})	ρ_m^{cal} /(g cm^{-3})	RD / %
0.0087	Water (1)+[C_4(3-m)Py][BF_4] (2)[49]	0.5965	318.15	1.1437	1.1441	0.04
0.0151	Water (1)+ [C_2MIm][BTI] (2)[50]	0.3025	298.19	1.5013	1.5002	-0.07
0.0102	Water (1)+ [empy][$EtSO_4$] (2)[51]	0.4972	298.15	1.20839	1.2081	-0.03
0.0028	Water (1)+ [C_6MIm][Cl] (2)[52]	0.5125	298.15	1.0422	1.0429	0.06
0.0062	Water (1)+ [C_6MIm][BF_4] (2)[53]	0.4861	298.15	1.13058	1.1312	0.05
0.0111	Water (1)+ [C_4MPyr][BTI] (2)[50]	0.2228	298.21	1.3871	1.3860	-0.08
0.0011	Water (1)+ [C_8MIm][Cl] (2)[52]	0.5334	298.15	1.0127	1.0120	-0.07
0.0093	Water (1)+ [pDMIM][BF_4] (2)[54]	0.4987	298.15	1.1998	1.2006	0.06
0.01	Water (1)+ [N_{1114}][BTI] (2) [50]	0.14	298.15	1.3895	1.3890	-0.04
0.0122	Methanol (1)+ [C_4MIm][SCN] (2)[55]	0.4917	298.15	1.0281	1.0283	0.02
0.0149	Ethanol (1)+ [Mmim][$MeSO_4$] (2)[56]	0.5000	298.15	1.1928	1.1933	0.04
0.0134	Ethanol (1)+ [C_4MIm][BF_4] (2)[57]	0.4976	298.15	1.1086	1.1092	0.06
0.0158	2-Propanol (1) + [MOA][BTI] (2)[58]	0.5176	298.15	1.0676	1.0669	-0.06
0.0134	2-Butanol (1) + [MOA][BTI] (2)[58]	0.4955	298.15	1.0667	1.0667	0.00
0.0167	Acetone (1)+ [C_4MIm][PF_6] (2)[50]	0.4993	298.15	1.2311	1.2320	0.07
0.0085	2-butanone (1)+ [Mmim][$MeSO_4$] (2)[59]	0.9994	298.15	0.8007	0.8002	-0.06
0.0137	2-butanone (1)+ [C_4MIm][PF_6] (2)[59]	0.5074	293.15	1.2116	1.2121	0.04
0.011	n-hexane (1)+ [C_8MIm][PF_6] (2)[60]	0.1268	298.15	1.2015	1.2018	0.03
0.0078	Methyl formate (1)+ [C_4MIm][BF_4] (2)[61]	0.5003	298.15	1.16043	1.1611	0.06
0.008	Methyl acetate (1)+ [C_4MIm][BF_4] (2)[61]	0.5007	298.15	1.13601	1.1368	0.07
0.0104	Ethyl acetate (1)+ [C_4MIm][PF_6] (2)[59]	0.5117	298.15	1.2266	1.2268	0.02
0.0058	Ethyl acetate (1)+ [Mmim][$MeSO_4$] (2)[59]	0.0928	298.15	1.3047	1.3058	0.08
0.0064	Dimethyl carbonate (1) +[C_6MIm][PF_6] (2)[62]	0.4957	298.15	1.2442	1.2446	0.03
-0.001	[C_6MIm][BF_4] (1)+[C_2MIm][BF_4] (2)[63]	0.5062	298.15	1.2006	1.2009	0.02
0.001	[C_4MIm][PF_6] (1) +[C_4MIm][BF_4] (2)[63]	0.4999	303.15	1.2846	1.2841	-0.04
0.001	[C_8MIm][Cl] (1)+[C_8MIm][BF_4] (2)[64]	0.6	313.15	1.0407	1.0410	0.02
0.0013	[C_6MIm][Cl] (1)+[C_6MIm][PF_6] (2)[64]	0.4	303.15	1.2005	1.2009	0.03
0.0058	Acetic acid (1) + [EMIM][$EtSO_4$] (2) [65]	0.4737	298.15	1.20174	1.2025	0.07
0.007	Propionic acid (1) + [EMIM][$EtSO_4$] (2) [65]	0.5516	298.15	1.16511	1.1661	0.08
0.0017	Acetic acid (1) + [BMIM][SCN] (2)[66]	0.5497	298.15	1.07098	1.0713	0.03
0.0032	Propionic acid (1) + [BMIM][SCN] (2) [66]	0.4978	298.15	1.05709	1.0578	0.06
0.0164	Acetonitrile (1) + [EMIM][$EtSO_4$] (2)[67]	0.4967	298.15	1.15023	1.1508	0.05
0.0115	Acetonitrile (1) + [BMIM][SCN] (2) [67]	0.4899	298.15	1.01748	1.0181	0.06

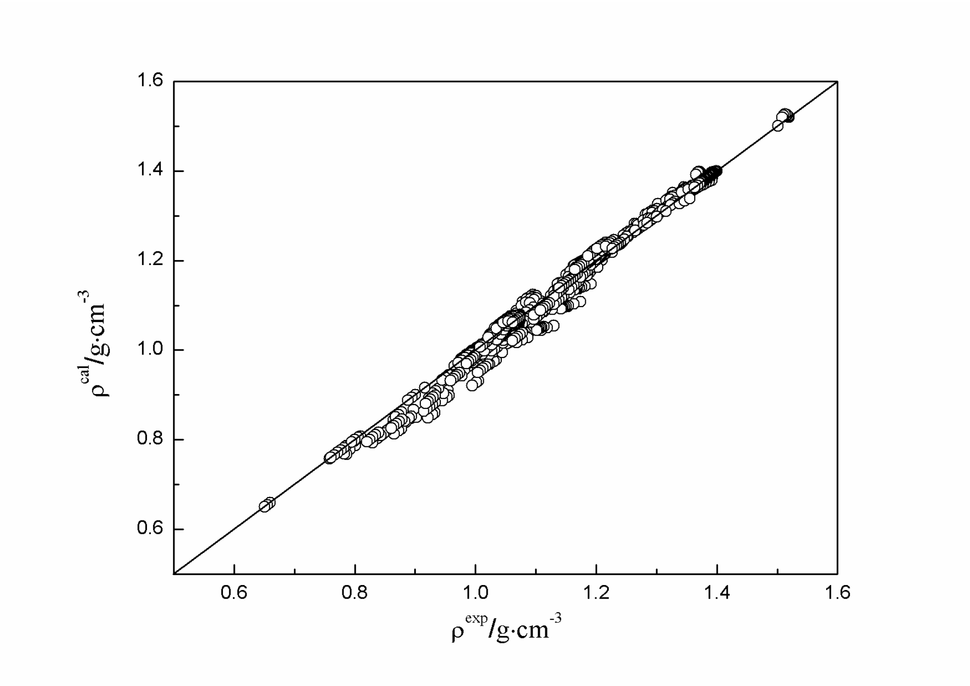

Figure 2. Experimental density of IL mixtures versus predicted value by the semi-empirical model (Eqs.1-2)

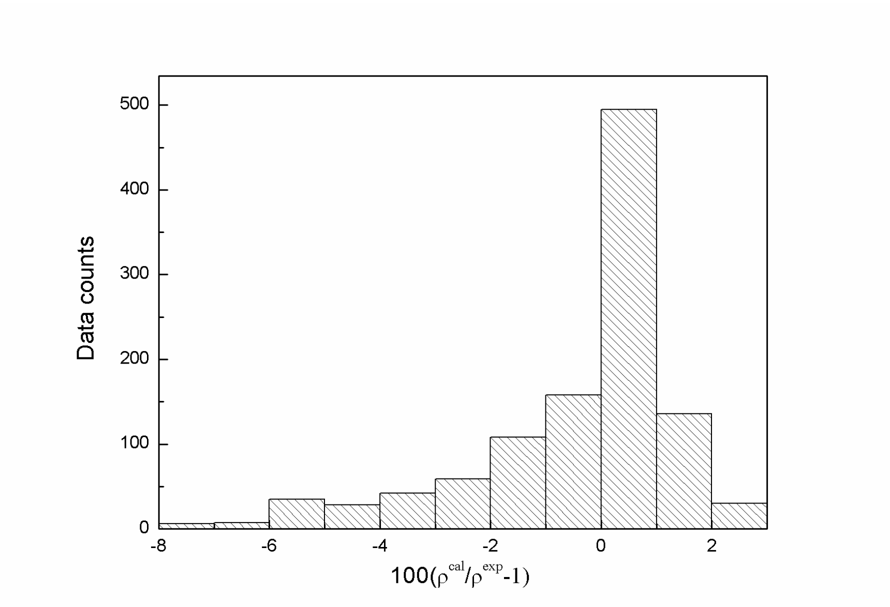

Figure 3. Histogram of relative deviations of predicted density by the semi-empirical model (Eqs.1-2)

Table 3. Predictive results of the semi-empirical model (Eqs.1-2) for density of IL mixtures

Binary system	x_1	*T*/ K	*N*p	Predicted deviations	
				AARD/ %	RD_{max} / %
Water (1)+[C_4(3-m)Py][BF_4] (2)[49]	0-1	293.15-318.15	65	1.76	-4.61
Water (1)+ [C_2MIm][BTI] (2)[50]	0-0.2032	298.19	7	0.55	0.89
Water (1)+ [empy][$EtSO_4$] (2)[51]	0-1	298.15-328.15	38	2.26	-6.62
Water (1)+ [C_6MIm][Cl] (2)[52]	0-1	298.15	10	0.55	-1.40
Water (1)+ [C_6MIm][BF_4] (2)[53]	0-1	298.15	17	0.76	-2.52
Water (1)+ [C_4MPyr][BTI] (2)[50]	0-0.9993	298.21-323.21	14	0.97	2.10
Water (1)+ [C_8MIm][Cl] (2)[52]	0-1	298.15-343.15	43	0.23	0.47
Water (1)+ [pDMIM][BF_4] (2)[54]	0-1	298.15-323.15	65	1.82	-5.43
Water (1)+ [N_{1114}][BTI] (2) [50]	0-0.2322	293.15-343.15	87	0.20	-0.84
Methanol (1)+ [C_4MIm][SCN] (2)[55]	0-1	298.15-328.15	50	2.42	-5.78
Ethanol (1)+ [Mmim][$MeSO_4$] (2)[56]	0-1	298.15	12	1.54	-3.36
Ethanol (1)+ [C_4MIm][BF_4] (2)[57]	0-1	298.15	13	1.73	-3.59
2-Propanol (1) + [MOA]+[BTI] (2)[58]	0.104-0.947	298.15-313.15	29	3.92	-7.85
2-Butanol (1) + [MOA]+[BTI] (2)[58]	0.0933-0.9306	298.15-313.15	29	2.8	-6.12
Acetone (1)+ [C_4MIm][PF_6] (2)[50]	0-1	298.15	14	1.94	-4.68
2-butanone (1)+ [Mmim][$MeSO_4$] (2)[59]	0-1	293.15-303.15	26	0.12	0.26
2-butanone (1)+ [C_4MIm][PF_6] (2)[59]	0-1	293.15-303.15	38	1.23	-2.81
n-hexane (1)+ [C_8MIm][PF_6] (2)[60]	0-1	293.15-303.15	17	0.05	0.09
Methyl formate (1)+ [C_4MIm][BF_4] (2)[61]	0-1	298.15	14	1.22	-2.80
Methyl acetate (1)+ [C_4MIm][BF_4] (2)[61]	0-1	298.15	14	1.09	-2.40
Ethyl acetate (1)+ [C_4MIm][PF_6] (2)[59]	0-1	293.15-303.15	38	0.85	-1.88
Ethyl acetate (1)+ [Mmim][$MeSO_4$] (2)[59]	0-1	293.15-303.15	20	0.06	0.15
Dimethyl carbonate (1) +[C_6MIm][PF_6] (2)[62]	0-1	298.15	12	0.84	-1.94
[C_6MIm][BF_4] (1)+[C_2MIm][BF_4] (2)[63]	0.0978-0.9455	298.15	12	0.03	0.06
[C_4MIm][PF_6] (1) +[C_4MIm][BF_4] (2)[63]	0.0568-0.945	303.15	11	0.46	-1.23
[C_8MIm][Cl] (1)+[C_8MIm][BF_4] (2)[64]	0.2-0.8	313.15	7	0.39	-0.63
[C_6MIm][Cl] (1)+[C_6MIm][PF_6] (2)[64]	0.2-0.8	303.15-333.15	15	0.04	0.08
Acetic acid (1) + [EMIM][$EtSO_4$] (2)[65]	0-1	298.15-313.15	59	0.94	-2.53
Propionic acid (1) + [EMIM][$EtSO_4$] (2) [65]	0-1	298.15-313.15	59	0.81	-1.92
Acetic acid (1) + [BMIM][SCN] (2)[66]	0-1	298.15-313.15	59	0.49	-1.44
Propionic acid (1) + [BMIM][SCN] (2) [66]	0-1	298.15-313.15	59	0.56	-1.56
Acetonitrile (1) + [EMIM][$EtSO_4$] (2)[67]	0-1	298.15-313.15	59	2.26	-5.59
Acetonitrile (1) + [BMIM][SCN] (2) [67]	0-1	298.15-313.15	59	1.63	-4.04
Overall	0-1	293.15-343.15	1071	1.1	-7.85

ANN model Figure 4 shows the comparison between the experimental density and predicted results by the ANN model. It can be seen that ANN also gave highly accurate prediction results with overall *AARD* of 0.42%. The relative deviations distribution was described in Figure 4. The ANN model provided more accurate predictive results with all the deviations less than ±3%.

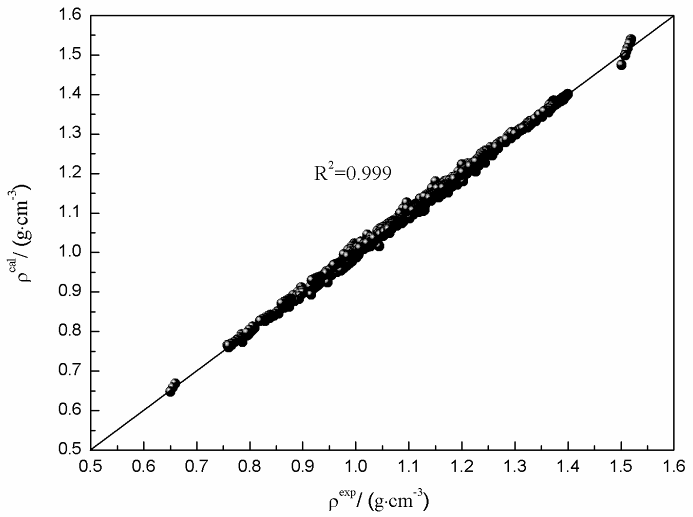

Figure 4. Experimental density of IL mixtures versus predicted value by the ANN model

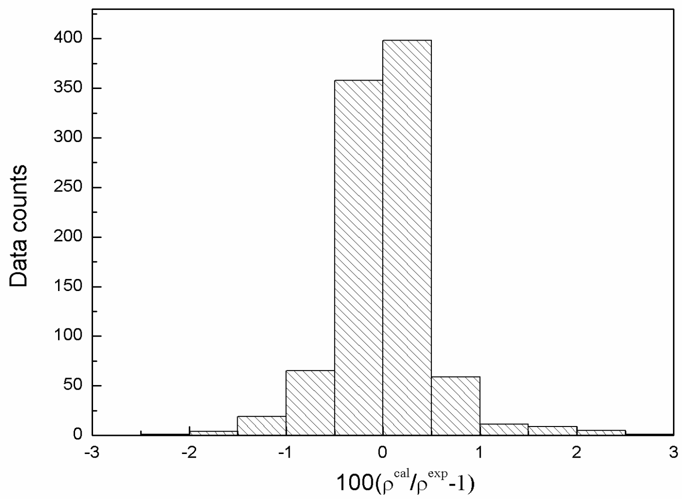

Figure 5. Histogram of relative deviations of predicted density by the ANN model

3.2 Prediction results of surface tension

Semi-empirical model Similar to the selection of dataset for density prediction, the 573 surface tension data points of 28 binary mixtures were also divided into correlation dataset (28 data points) and validation dataset (545 data points). Table 4 provides the correlation results with all the relative deviations less than ±0.1%, which indicates highly accurate correlation results by the semi-empirical model for surface tension.

Table 4. Correlated results of the semi-empirical model for surface tension of IL mixtures (Eqs.3-5)

Parameter *b* or *b'*	Binary system	x_1	*T*/ K	σ_m^{exp} /(mN m^{-1})	σ_m^{cal} /(mN m^{-1})	*RD* / %
-0.0080	Water (1)+ $[C_2MIm][BF_4]$ (2)[57]	0.4926	298.15	53.88	53.88	0.00
-0.0124	Water (1)+ $[C_4MIm][BF_4]$ (2)[57]	0.4696	298.15	46.02	45.95	0.06
-0.0180	Water (1)+ $[C_6MIm][BF_4]$ (2)[57]	0.4942	298.15	37.65	37.65	0.00
-0.0013	Water (1)+ $[C_1MIm][MeSO_4]$ (2)[68]	0.7080	298.1	64.70	64.70	0.00
-0.0023	Water (1)+ $[C_2MIm][MeSO_3]$ (2)[68]	0.5150	301.7	58.10	58.14	0.07
-0.0096	Water (1)+ $[C_2MIm][EtSO_4]$ (2)[69]	0.5161	298.15	48.97	49.01	0.08
-0.0164	Water (1)+ $[C_2MIm][C4SO_4]$ (2)[32]	0.5008	298.15	40.01	40.05	0.09
-0.0055	Water (1)+ $[C_4MIm][Gly]$ (2)[70]	0.1358	298.15	45.90	45.88	0.05
-0.0148	Water (1)+ $[C_4Py][NO_3]$ (2)[71]	0.6753	298.15	44.00	44.03	0.07
-0.0114	Water (1)+ $[N_{311}(hoe)][Br]$ (2)[72]	0.9953	298.15	48.30	48.27	0.06
-0.0031	Water (1)+ $[N_{112}(hoe)][Br]$ (2)[72]	0.9953	298.15	65.23	65.22	0.01
-0.0213	Water (1)+ $[P_{666(14)}][Dca]$ (2)[73]	0.4932	328	30.50	30.52	0.06
-0.0295	Water (1)+ $[P_{666(14)}][BTI]$ (2)[73]	0.0891	318	28.60	28.61	0.03
-0.0102	Methanol (1)+ $[C_1MIm][MeSO_4]$ (2)[72]	0.5214	298.15	36.75	36.75	0.00
0.0153	Methanol (1)+ $[C_2MIm][MeSO_4]$ (2)[74]	0.5988	298.15	37.21	37.22	0.03
-0.0164	Ethanol (1)+ $[C_4MIm][BF_4]$ (2)[57]	0.4976	298.15	28.87	28.88	0.04
-0.0034	Ethanol (1)+ $[C_6MIm][BF_4]$ (2)[57]	0.4921	298.15	28.82	28.83	0.03
0.0020	Ethanol (1)+ $[C_8MIm][BF_4]$ (2)[57]	0.4875	298.15	27.90	27.92	0.08
0.0066	Ethanol (1)+ $[C_2MIm][C_6SO_4]$ (2)[32]	0.5309	298.15	29.48	29.49	0.05
0.0120	Ethanol (1)+ $[C_2MIm][C_8SO_4]$ (2)[32]	0.4941	298.15	29.14	29.15	0.03
0.0015	1-propanol (1)+ $[C_4MIm][BTI]$ (2)[75]	0.4830	298.15	28.60	28.59	0.03
-0.0064	1-butanol (1)+ $[C_4MIm][BTI]$ (2)[75]	0.4998	298.15	26.79	26.81	0.07
0.0034	Tetrahydrofuran (1)+ $[C_2MIm][BTI]$ (2)[76]	0.4531	298.15	32.63	32.64	0.03
0.0048	Tetrahydrofuran (1)+ $[C_4MIm][BTI]$ (2)[77]	0.5103	298.15	30.75	30.75	0.01
0.0091	Acetonitrile (1)+ $[C_2MIm][BTI]$ (2)[76]	0.5276	298.15	34.42	34.44	0.07
0.0071	Acetonitrile (1)+ $[C_4MIm][BTI]$ (2)[77]	0.5290	298.15	32.15	32.16	0.05
-0.0083	Dimethyl sulfoxide (1)+ $[C_2MIm][BTI]$ (2)[77]	0.4914	298.15	36.49	36.46	0.07
-0.0121	Dimethyl sulfoxide (1)+ $[C_4MIm][BTI]$ (2)[77]	0.5215	298.15	33.96	33.94	0.05

Figure 6 shows the further prediction results using the semi-empirical model (Eqs.3-5) and correlated parameters (see Table 4). It can be seen that data points distributed closely along the solid line of $\sigma^{cal}=\sigma^{exp}$, which indicates the good predictIve performance of the surface tension model. Furthermore, the relative deviations against the mole fraction of water and organics were described in Figure 7. It can be seen that 74.5% of the deviations were within ±2%, and only 4.6% were higher than ±4%. Detailed prediction deviations of each binary system were summarized in Table 5, and the overall *AARD* was 1.55%. After comparing different kinds of binary systems, it can be concluded that the water + [C_nMIm][BF_4] and tetrahydrofuran + [C_2MIm][BTI] system present relatively higher prediction accuracy. However, water-based IL mixtures produce lower prediction accuracy. This may be caused by the low prediction performance of the semi-empirical model at high content of water. Compared to the previous reviewed models, the current semi-empirical model for surface tension presents higher prediction accuracy and requires less adjustable parameter.

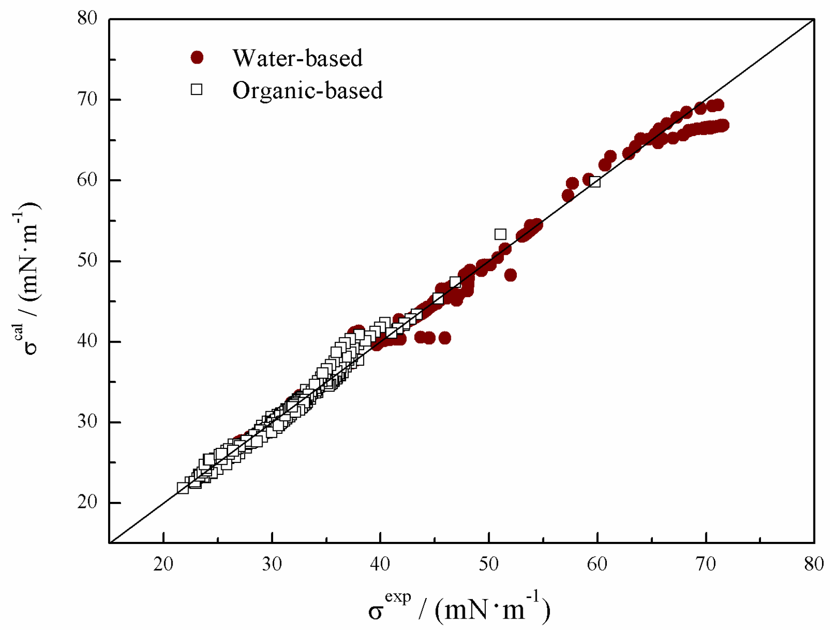

Figure 6. Experimental surface tension of IL mixtures versus predicted value by the semi-empirical model (Eqs.3-5)

Table 5. Predictive results of the semi-empirical model (Eqs.3-5)for surface tension of IL mixtures

Binary system	x_1	*T*/ K	*N*p	Predicted deviations	
				AARD/ %	RD_{max}/ %
Water (1)+ [C_2MIm][BF_4] (2)[57]	0-0.8582	298.15	8	0.21	1.08
Water (1)+ [C_4MIm][BF_4] (2)[57]	0-0.8987	298.15	14	0.58	1.96
Water (1)+ [C_6MIm][BF_4] (2)[57]	0-0.6968	298.15	7	0.22	-0.39
Water (1)+ [C_1MIm][$MeSO_4$] (2)[68]	0.7390-1	296.8-298.1	9	1.06	-2.41
Water (1)+ [C_2MIm][$MeSO_3$] (2)[68]	0.5260-1	300-303.3	26	4.04	-6.63
Water (1)+ [C_2MIm][$EtSO_4$] (2)[69]	0.0062 -0.5791	298.15	11	1.73	-3.93
Water (1)+ [C_2MIm][C_4SO_4] (2)[32]	0-0.9611	298.15	26	2.11	-11.96
Water (1)+ [C_4MIm][Gly] (2)[70]	0-0.1358	283.15-328.15	59	0.36	-0.96
Water (1)+ [C_4Py][NO_3] (2)[71]	0-0.9903	298.15	14	3.98	9.31
Water (1)+ [N_{311}(hoe)][Br] (2)[72]	0.9900-0.9979	298.15	2	4.16	-7.16
Water (1)+ [N_{112}(hoe)][Br] (2)[72]	0.9915-0.9981	298.15	2	2.21	-2.56
Water (1)+ [$P_{666(14)}$][Dca] (2)[73]	0.4932	298.2-342.8	5	1.49	2.36
Water (1)+ [$P_{666(14)}$][BTI] (2)[73]	0.0891	298.1-343.3	5	1.70	2.47
Methanol (1)+ [C_1MIm][$MeSO_4$] (2)[72]	0-1	298.15	8	1.18	4.33
Methanol (1)+ [C_2MIm][$MeSO_4$] (2)[74]	0.6976-1	298.15	6	0.71	2.48
Ethanol (1)+ [C_4MIm][BF_4] (2)[57]	0-0.9014	298.15	11	0.76	-1.78
Ethanol (1)+ [C_6MIm][BF_4] (2)[57]	0-0.9020	298.15	9	0.70	-1.50
Ethanol (1)+ [C_8MIm][BF_4] (2)[57]	0-0.8988	298.15	9	0.91	-1.85
Ethanol (1)+ [C_2MIm][C_6SO_4] (2)[32]	0-0.9700	298.15	12	1.69	-3.41
Ethanol (1)+ [C_2MIm][C_8SO_4] (2)[32]	0-0.9601	298.15	17	1.95	-4.20
1-propanol (1)+ [C_4MIm][BTI] (2)[75]	0-1	298.15	10	1.48	3.05
1-butanol (1)+ [C_4MIm][BTI] (2)[75]	0-1	298.15	12	2.59	4.84
Tetrahydrofuran (1)+ [C_2MIm][BTI] (2)[76]	0-1	293.15-308.15	43	0.47	-1.47
Tetrahydrofuran (1)+ [C_4MIm][BTI] (2)[77]	0-1	293.15-308.15	39	0.60	2.60
Acetonitrile (1)+ [C_2MIm][BTI] (2)[76]	0-1	293.15-313.15	44	1.13	-3.32
Acetonitrile (1)+ [C_4MIm][BTI] (2)[77]	0-1	293.15-313.15	44	1.36	-4.16
Dimethyl sulfoxide (1)+ [C_2MIm][BTI] (2)[77]	0-1	293.15-313.15	44	1.63	4.41
Dimethyl sulfoxide (1)+ [C_4MIm][BTI] (2)[77]	0-1	293.15-313.15	49	2.34	7.87
Overall	0-1	293.15-343.3	545	1.55	-11.96

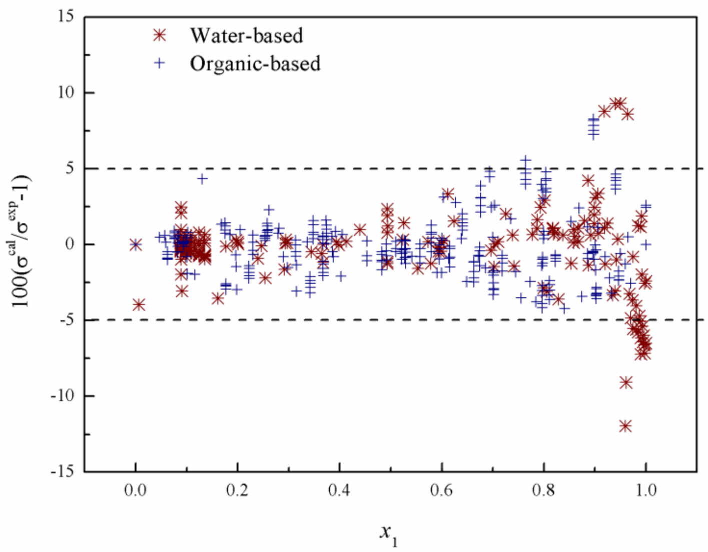

Figure 7. Predicted relative deviations from the semi-empirical model (Eqs.3-5) against the mole fraction of molecular solvents in water-based and organic-based IL mixtures.

ANN model Figure 8 shows the predicted results from the two ANN models for surface tension of water-based and organic-based IL mixtures. Relative deviation of training, validation and test subsets were illustrated in Figure 9. There were 97% and 95% of the deviations within ±2% for water-based and organic-based IL mixtures, respectively. The maximum deviation was found to be -11.6% of the mixture of water and $[C_4Py][NO_3]$ at x_{water}=0.9903, which probably can be attributed to two factors, namely (1) the random error of trained ANN model at high water content, and (2) the inaccuracy of the experimental data, since there were many other deviations at high water content within ±2%. In general, the above results indicate that the ANN models can be successfully applied in predicting the surface tensions of IL mixtures.

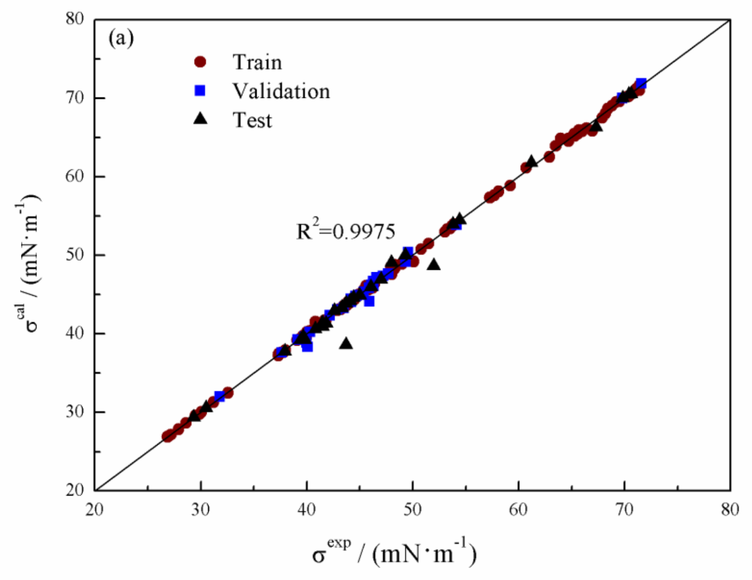

1

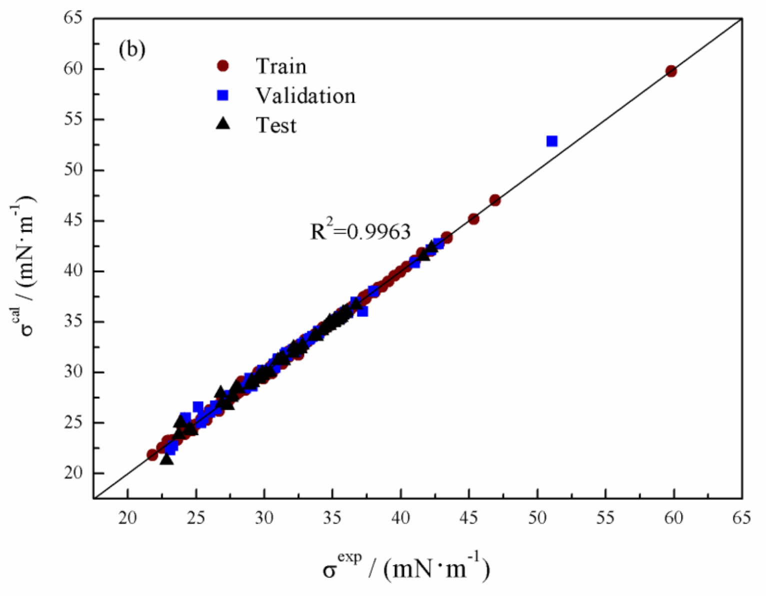

2

3 Figure 8. Predicted results by ANN models versus experimental data of surface tensions of

4 water-based IL mixtures (a) and organic-based IL mixtures (b).

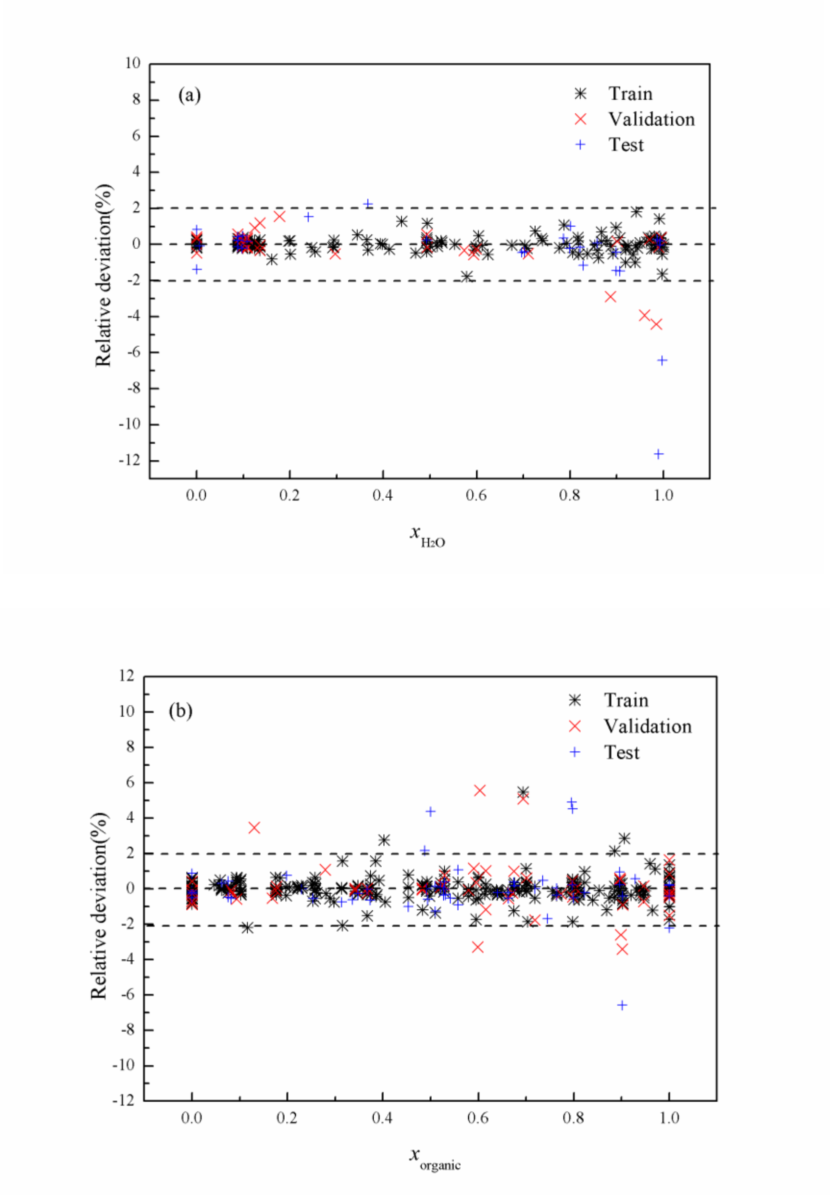

Figure 9. Relative deviation of training, validation and test subsets against the mole fraction of molecular solvents in water-based IL mixtures (a) and organic-based IL mixtures (b).

3.3 Prediction results of heat capacity

Semi-empirical model similar to the prediction of density and surface tension, 603 heat capacity data points of 9 binary mixtures were also divided into correlation dataset (9 data points) and validation dataset (594 data points). All the correlation deviation of each mixture were within ±0.1%, as shown in Table 6. Based on the correlated parameters, further prediction of heat capacity was performed. The comparison between the predicted and experimental data of heat capacity was shown in Figure 10 with the overall *AARD* of 0.93%.

It was observed that the semi-empirical model gave highly accurate prediction results. Furthermore, the histogram of the relative deviations was given in Figure 11. It can be seen that more than 75% of the relative deviations were within ±1%, and only 6% were in the range between ±3% and ±6%. Predictive *AARD* of each binary system was listed in Table 7. All the *AARD*s are less than 3% and the maximum relative deviation is -5.75%, which indicates the semi-empirical model also has high accuracy in predicting heat capacity of IL mixtures.

Table 6. Correlated results of the semi-empirical model for heat capacity of IL mixtures (Eqs.6-7)

Parameter c	Binary system	x_1	T/ K	C_{pm}^{exp} / (J mol^{-1} K^{-1})	C_{pm}^{cal} /(J mol^{-1} K^{-1})	RD / %
0.00445	Water (1)+ [C_4MIm][BF_4] (2)[34]	0.4000	303.2	259.4	259.4	0.02
-0.0026	Water (1)+ [C_4MIm][PF_6] (2)[34]	0.2000	303.2	342.2	342.0	-0.05
-0.00005	Water (1)+ [C_4MIm][TfO] (2)[35]	0.4000	303.2	295	295.2	0.05
0.0019	Water (1)+ [C_4MIm][$MeSO_4$] (2)[35, 78]	0.4000	303.2	265	265.1	0.03
-0.0007	Acetonitrile (1)+ [C_6MIm][BF_4] (2)[79]	0.4633	298.15	272.6	272.4	-0.07
-0.0008	Acetonitrile (1)+ [C_8MIm][BF_4] (2)[79]	0.4563	298.15	310.5	310.4	-0.03
0.00185	Methanol (1)+ [C_6MIm][BF_4] (2)[80]	0.6030	298.15	223.9	224.0	0.07
0.0014	Methanol (1)+ [C_8MIm][BF_4] (2)[80]	0.5484	298.15	273.5	273.6	0.03
0.00135	Ethanol (1)+ [bmpyr][BF_4] (2)[49]	0.4969	298.15	254.2	254.3	0.03

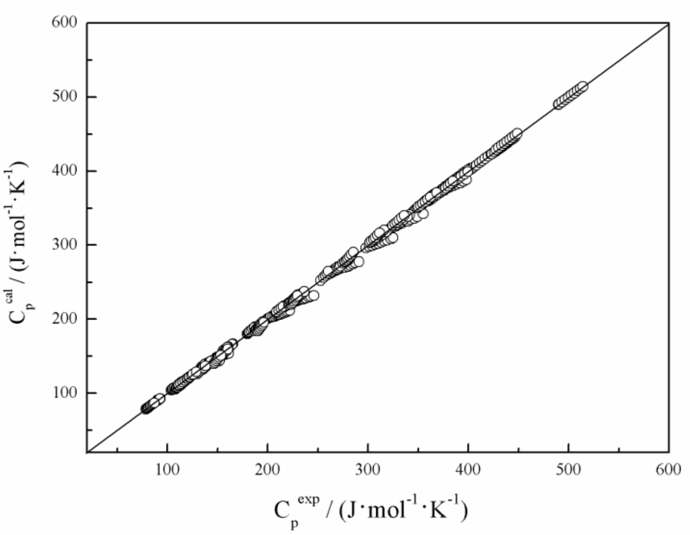

Figure 10. Experimental heat capacity of IL mixtures versus predicted value by the semi-empirical model (Eqs.6-7)

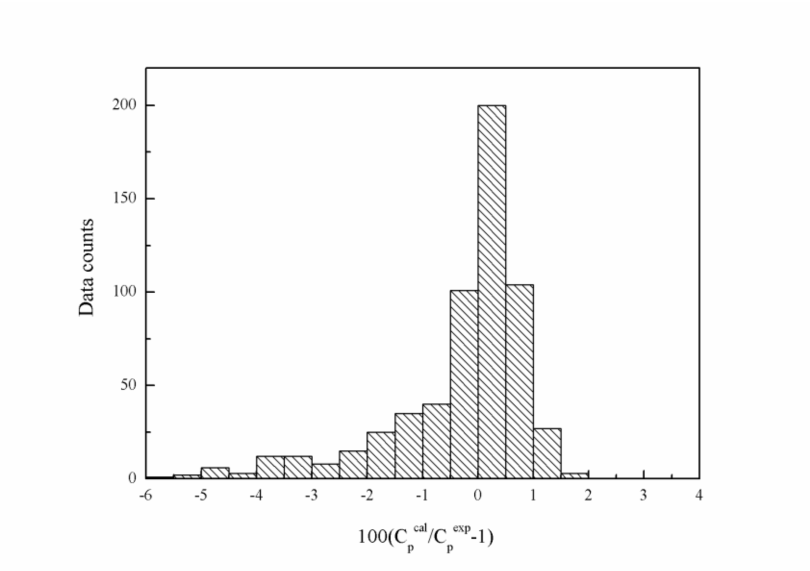

Figure 11. Histogram of relative deviations of predicted heat capacity by the semi-empirical model (Eqs.6-7)

Table 7. Predicted results of the semi-empirical model for heat capacity of IL mixtures

Binary system	x_1	T/ K	Np	Predicted deviations	
				AARD/ %	RD_{max}/ %
Water (1)+ $[C_4MIm][BF_4]$ (2)[34]	0.2-0.8	303.2-353.2	43	0.6	-1.64
Water (1)+ $[C_4MIm][PF_6]$ (2)[34]	0.05-0.2	308.2-353.2	43	0.2	0.61
Water (1)+ $[C_4MIm][TfO]$ (2)[35]	0.2-0.8	303.2-353.2	43	2.2	-5.75
Water (1)+ $[C_4MIm][MeSO_4]$ (2)[35, 78]	0.2-0.8	303.2-353.2	42	2.5	-5.05
Acetonitrile (1)+ $[C_6MIm][BF_4]$ (2)[79]	0-1	283.15-323.15	89	0.3	0.98
Acetonitrile (1)+ $[C_8MIm][BF_4]$ (2)[79]	0-1	283.15-323.15	98	0.5	1.39
Methanol (1)+ $[C_6MIm][BF_4]$ (2)[80]	0-1	283.15-323.15	70	0.7	-2.26
Methanol (1)+ $[C_8MIm][BF_4]$ (2)[80]	0-1	283.15-323.15	71	0.6	-2.03
Ethanol (1)+ $[bmpyr][BF_4]$ (2)[49]	0-1	293.15-318.15	95	0.8	-4.46
Overall	0-1	283.15-353.2	594	0.93	-5.75

ANN model The comparison between the experimental heat capacity and calculated value by the ANN model was shown in Figure 12. The histogram of the relative deviations was given in Figure 13. It can be seen from the Figures that ANN model provided more accurate predictive results with all the absolute deviations less than 1.2%.

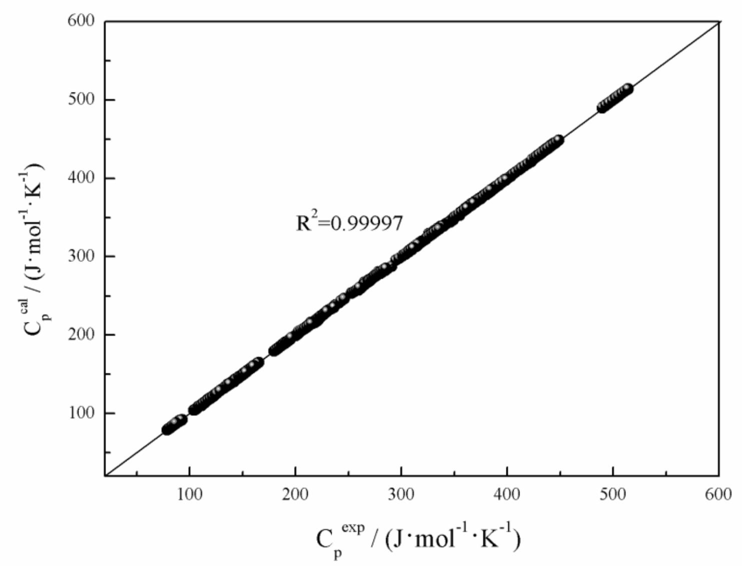

Figure 12. Experimental heat capacity of IL mixtures versus predicted value by the ANN model

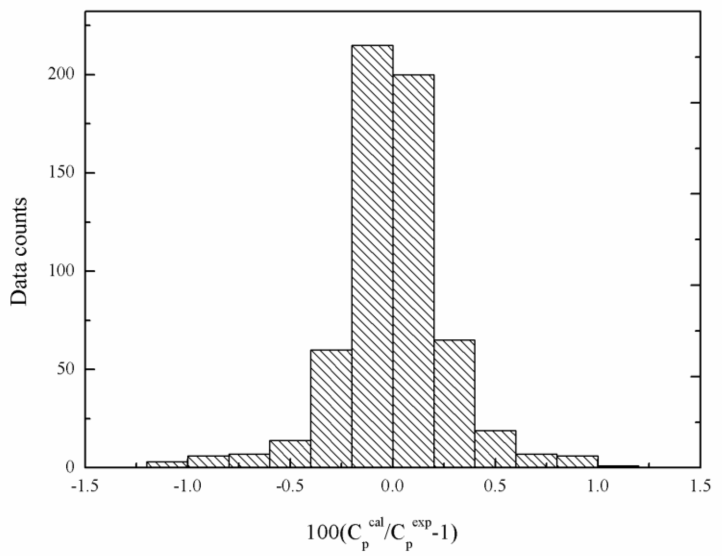

Figure 13. Histogram of relative deviations of predicted heat capacity by the ANN model

3.4 Prediction results of thermal conductivity

Experimental data of thermal conductivity were rarely found in literature, thus only 24 data points of 3 binary mixtures were collected to verify the models. Correlation deviation of each mixture was within ±0.1%, as shown in Table 8. With the semi-empirical model (Eqs.8-9) and parameter *d*, thermal conductivity of the other 21 data points were predicted and depicted in Figure 14. Detailed results of each mixture were listed in Table 9. The overall *AARD* was 1.9%, which indicates the semi-empirical model for is useful in predicting thermal conductivity of IL mixtures. In addition, the ANN model gave higher accurate prediction results with overall *AARD* of 0.4%, as shown in Figure 15.

Table 8. Correlated results of the semi-empirical model for thermal conductivity of IL mixtures (Eqs.8-9)

Parameter *d*	Binary system	w_1	*T*/ K	λ_m^{exp} / (W m^{-1} K^{-1})	λ_m^{cal} /(W m^{-1} K^{-1})	*RD* / %
-0.0301	Water (1)+ [C_2mim][$EtSO_4$] (2)[81]	0.20	293	0.232	0.2322	0.07
-0.018	Water (1)+ [C_4MIm][TfO] (2)[81]	0.20	293	0.221	0.2209	-0.06
-0.003	Methanol (1)+ [Mmim][DMP] (2)[82]	0.2518	298.15	0.222	0.2219	-0.03

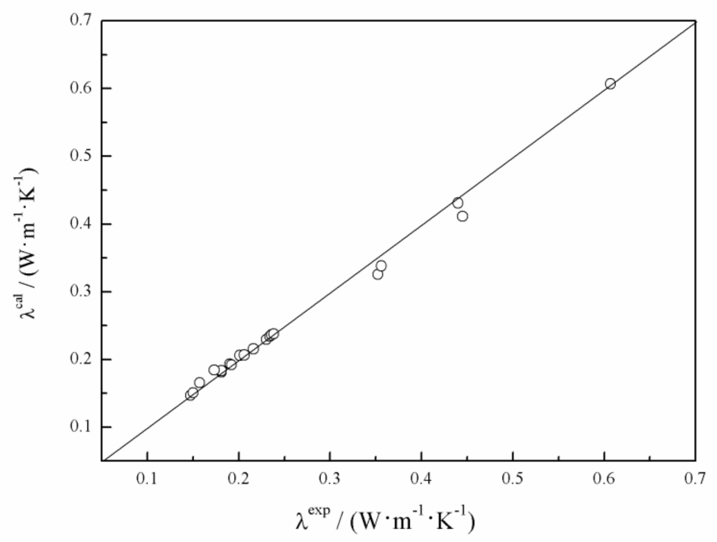

Figure 14. Predicted results by the semi-empirical model (Eqs.8-9) versus experimental data of thermal conductivity.

Table 9. Predicted results of the semi-empirical model for thermal conductivity of IL mixtures (Eqs.8-9)

Binary system	w_1	*T*/ K	*N*p	Predicted deviations	
				AARD/ %	RD_{max}/ %
Water (1)+ [C_2mim][$EtSO_4$] (2)[81]	0-1	293	7	2.94	-7.57
Water (1)+ [C_4MIm][TfO] (2)[81]	0-1	293	7	2.77	6.43
Methanol (1)+ [Mmim][DMP] (2)[82]	0-1	298.15	7	0.09	-0.20
Overall	0-1	293-298.15	21	1.9	-7.57

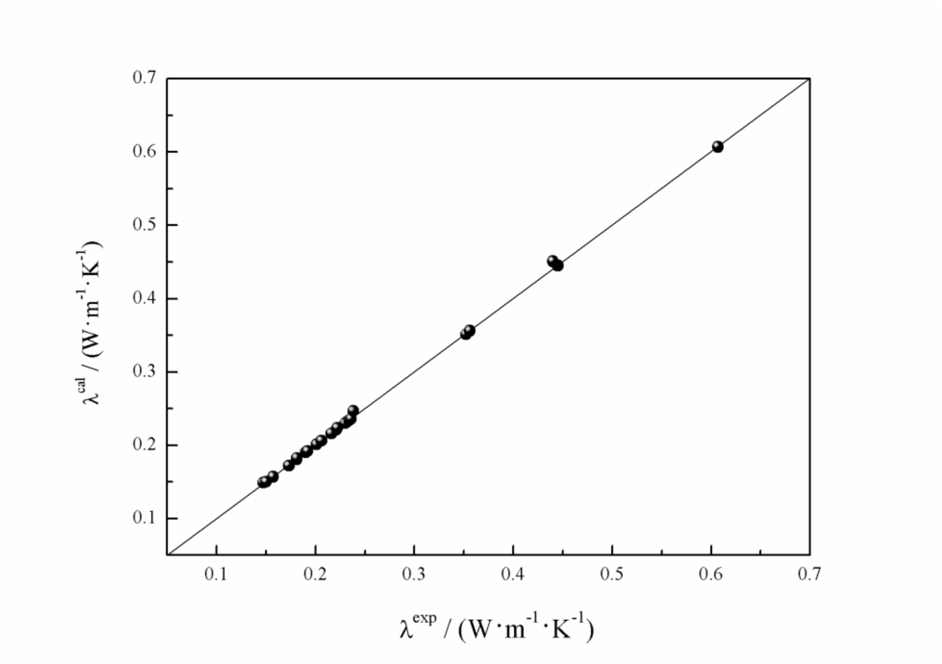

Figure 15. Predicted results by ANN model versus experimental data of thermal conductivity.

4 Conclusions

This paper provides semi-empirical models and ANN models to predict thermophysical properties of IL mixtures involving molecular compounds. Each semi-empirical model only contain one characteristic parameter, which can be determined by one experimental data. These models and parameters were checked by 659 data points of density, 545 data points of surface tension, 594 data points of heat capacity and 21 data points of thermal conductivity. The proposed semi-empirical models present accurate predictive results with the overall *AARD*s less than 2%. Compared to the previous reported methods in Table 1, the semi-empirical models present equivalent accuracy and are verified by more kinds of IL mixtures. Besides, the semi-empirical models require only one parameter, which would be more convenient to use. The more accurate predicted results from the ANN models than the semi-empirical models have verified ANN as an effective tool in predicting thermophysical properties of IL mixtures. Even so, the semi-empirical models are better alternative because they provide specific thermophysical equations and can be used directly without any computer-aided program.

Supplementary Material

The predicted results of density, surface tension, heat capacity and thermal conductivity were given here, including the constant *a*, *b*(*b'*), *c* and *d* values of each IL mixture, the full name and molar fraction of each component, experimental and calculated properties of all the mixtures by the semi-empirical models and ANN models.

Acknowledgments

This research was supported by the National Natural Science Fund for Distinguished Young Scholars (21425625), the National Basic Research Program of China (973 Program) (2013CB733506, 2015CB251403) and the key program of Beijing Municipal Natural Science Foundation (2141003). We also appreciate the support from the Science and Technology Innovation Team of Cross and Cooperation of Chinese Academy of Sciences.

References

1 D. R. MacFarlane and K. R. Seddon, *Aust. J. Chem.*, 2007, **60**, 3-5.
2 M. J. Earle and K. R. Seddon, *Pure Appl. Chem.*, 2000, **72**, 1391-1398.
3 Y. Huang, H. Dong, X. Zhang, C. Li and S. Zhang, *AIChE J.*, 2013, **59**, 1348-1359.
4 J. Palomar, V. R. Ferro, J. S. Torrecilla and F. Rodríguez, *Ind. Eng. Chem. Res.*, 2007, **46**, 6041-6048.
5 J. A. P. Coutinho, P. J. Carvalho and N. M. C. Oliveira, *RSC Adv.*, 2012, **2**, 7322-7346.
6 V. H. Alvarez, S. Mattedi, M. Martin-Pastor, M. Aznar and M. Iglesias, *J. Chem. Thermodyn.*, 2011, **43**, 997-1010.
7 A. E. Andreatta, E. Rodil, A. Arce and A. Soto, *J. Solut. Chem.*, 2014, 1-17.
8 S. M. Hosseini, M. M. Papari, F. Fadaei-Nobandegani and J. Moghadasi, *J. Solut. Chem.*, 2013, **42**, 1854-1862.
9 S. M. Hosseini, J. Moghadasi, M. M. Papari and F. Fadaei Nobandegani, *Ind. Eng. Chem. Res.*, 2011, **51**, 758-766.
10 F. Yousefi, *Ionics*, 2012, **18**, 769-775.
11 P.-Y. Lin, A. N. Soriano, R. B. Leron and M.-H. Li, *Exp. Therm. Fluid. Sci.*, 2011, **35**, 1107-1112.
12 I. Bahadur and N. Deenadayalu, *J. Solut. Chem.*, 2011, **40**, 1528-1543.
13 I. Bahadur, N. Deenadayalu, P. Naidoo and D. Ramjugernath, *J. Chem. Thermodyn.*, 2013, **57**, 203-211.
14 O. REDLLICH and A. Kister, *Ind. Eng. Chem.*, 1948, **40**, 345-348.
15 V. Govinda, P. Attri, P. Venkatesu and P. Venkateswarlu, *J. Phys. Chem. B*, 2013, **117**, 12535-12548.
16 G. Zuo, Z. Zhao, S. Yan and X. Zhang, *Chem. Eng. J.*, 2010, **156**, 613-617.
17 I. M. S. Lampreia, F. A. Dias and A. F. S. S. Mendonca, *Phys. Chem. Chem. Phys.*, 2003, **5**, 4869-4874.
18 N. Deenadayalu, I. Bahadur and T. Hofman, *J. Chem. Thermodyn.*, 2010, **42**, 726-733.
19 N. Deenadayalu, I. Bahadur and T. Hofman, *J. Chem. Eng. Data*, 2011, **56**, 1682-1686.
20 V. Govinda, P. Madhusudhana Reddy, I. Bahadur, P. Attri, P. Venkatesu and P. Venkateswarlu, *Thermochim. Acta*, 2013, **556**, 75-88.
21 H. Rawson, *Properties and applications of glass*, North-Holland, 1980.
22 S. Singh, M. Aznar and N. Deenadayalu, *J. Chem. Thermodyn.*, 2013, **57**, 238-247.
23 I. Polishuk, *J. Supercrit. Fluid.*, 2012, **67**, 94-107.
24 R. Sedev, *Curr. Opin. Colloid Interface Sci.*, 2011, **16**, 310-316.
25 M. Tariq, M. G. Freire, B. Saramago, J. A. P. Coutinho, J. N. C. Lopes and L. P. N. Rebelo, *Chem. Soc. Rev.*, 2012, **41**, 829-868.
26 R. L. Gardas and J. A. Coutinho, *Fluid Phase Equilibr.*, 2008, **265**, 57-65.

27 M. Deetlefs, K. R. Seddon and M. Shara, *Phys. Chem. Chem. Phys.*, 2006, **8**, 642-649.
28 M. Mousazadeh and E. Faramarzi, *Ionics*, 2011, **17**, 217-222.
29 R. L. Gardas, R. Ge, N. Ab Manan, D. W. Rooney and C. Hardacre, *Fluid Phase Equilibr.*, 2010, **294**, 139-147.
30 D. Fu, H. Wang and L. Du, *J. Chem. Thermodyn.*, 2014, **71**, 1-5.
31 Y. Xu, H. Zhu and L. Yang, *J. Chem. Eng. Data*, 2013, **58**, 2260-2266.
32 E. Rilo, M. Domínguez-Pérez, J. Vila, L. M. Varela and O. Cabeza, *J. Chem. Thermodyn.*, 2012, **49**, 165-171.
33 E. Ghasemian Lemraski and Z. Pouyanfar, *J. Chem. Eng. Data*, 2014, **59**, 3982-3987.
34 Y.-H. Yu, A. N. Soriano and M.-H. Li, *J. Taiwan Inst. Chem. E.*, 2009, **40**, 205-212.
35 P.-Y. Lin, A. N. Soriano, A. R. Caparanga and M.-H. Li, *Thermochim. Acta*, 2009, **496**, 105-109.
36 H. Parhizgar, M. R. Dehghani, A. Khazaei and M. Dalirian, *Ind. Eng. Chem. Res.*, 2012, **51**, 2775-2781.
37 K. Shahbaz, S. Baroutian, F. S. Mjalli, M. A. Hashim and I. M. AlNashef, *Thermochim. Acta*, 2012, **527**, 59-66.
38 M. Moosavi and N. Soltani, *Fluid Phase Equilibr.*, 2013, **356**, 176-184.
39 J. S. Torrecilla, F. Rodriguez, J. L. Bravo, G. Rothenberg, K. R. Seddon and I. Lopez-Martin, *Phys. Chem. Chem. Phys.*, 2008, **10**, 5826-5831.
40 J. O. Valderrama, A. Reátegui and R. E. Rojas, *Ind. Eng. Chem. Res.*, 2009, **48**, 3254-3259.
41 N. V. K. Dutt, Y. V. L. Ravikumar and K. Y. Rani, *Chem. Eng. Commun.*, 2013, **200**, 1600-1622.
42 M.-R. Fatehi, S. Raeissi and D. Mowla, *Fluid Phase Equilibr.*, 2014, **364**, 88-94.
43 M. Lashkarbolooki, A. Z. Hezave and S. Ayatollahi, *Fluid Phase Equilibr.*, 2012, **324**, 102-107.
44 A. Z. Hezave, S. Raeissi and M. Lashkarbolooki, *Ind. Eng. Chem. Res.*, 2012, **51**, 9886-9893.
45 J. R. Brock and R. B. Bird, *AIChE J.*, 1955, **1**, 174-177.
46 I. Jahanandish, B. Salimifard and H. Jalalifar, *J. Petrol. Sci. Eng.*, 2011, **75**, 336-342.
47 K. Levenberg, *Q. Appl. Math.*, 1944, **2**, 164-168.
48 M. T. Hagan and M. B. Menhaj, *Neural Networks, IEEE Transactions on*, 1994, **5**, 989-993.
49 G. García-Miaja, J. Troncoso and L. Romaní, *J. Chem. Eng. Data*, 2007, **52**, 2261-2265.
50 S. Wang, J. Jacquemin, P. Husson, C. Hardacre and M. F. Costa Gomes, *J. Chem. Thermodyn.*, 2009, **41**, 1206-1214.
51 B. González, N. Calvar, E. Gómez, E. A. Macedo and Á. Domínguez, *J. Chem. Eng. Data*, 2008, **53**, 1824-1828.
52 E. Gómez, B. González, Á. Domínguez, E. Tojo and J. Tojo, *J. Chem. Eng. Data*, 2006, **51**, 696-701.
53 A. Stoppa, J. Hunger and R. Buchner, *J. Chem. Eng. Data*, 2008, **54**, 472-479.
54 M.-L. Ge, X.-G. Ren, Y.-J. Song and L.-S. Wang, *J. Chem. Eng. Data*, 2009, **54**, 1400-1402.
55 H. Rodríguez and J. F. Brennecke, *J. Chem. Eng. Data*, 2006, **51**, 2145-2155.
56 E. Gómez, B. González, N. Calvar and Á. Domínguez, *J. Chem. Thermodyn.*, 2008, **40**, 1208-1216.
57 E. Rilo, J. Pico, S. García-Garabal, L. M. Varela and O. Cabeza, *Fluid Phase Equilibr.*, 2009, **285**, 83-89.
58 I. Bahadur, N. Deenadayalu, Z. Tywabi, S. Sen and T. Hofman, *J. Chem. Thermodyn.*, 2012, **49**, 24-38.
59 A. B. Pereiro and A. Rodríguez, *J. Chem. Eng. Data*, 2007, **52**, 600-608.
60 A. Pereiro and A. Rodriguez, *Phys. Chem. Liq.*, 2008, **46**, 162-174.
61 Y. Tian, X. Wang and J. Wang, *J. Chem. Eng. Data*, 2008, **53**, 2056-2059.
62 A. Pereiro, E. Tojo, A. Rodrıguez, J. Canosa and J. Tojo, *J. Chem. Thermodyn.*, 2006, **38**, 651-661.
63 P. Navia, J. Troncoso and L. Romaní, *J. Chem. Eng. Data*, 2007, **52**, 1369-1374.
64 H. Ning, M. Hou, Q. Mei, Y. Liu, D. Yang and B. Han, *Sci. China Chem.*, 2012, **55**, 1509-1518.
65 S. Singh, I. Bahadur, G. G. Redhi, E. E. Ebenso and D. Ramjugernath, *J. Mol. Liq.*, 2014, **199**, 518-523.
66 S. Singh, I. Bahadur, G. G. Redhi, E. E. Ebenso and D. Ramjugernath, *J. Chem. Thermodyn.*, 2015, **89**, 104-111.
67 S. Singh, I. Bahadur, G. G. Redhi, D. Ramjugernath and E. E. Ebenso, *J. Mol. Liq.*, 2014, **200, Part B**, 160-167.
68 J. W. Russo and M. M. Hoffmann, *J. Chem. Eng. Data*, 2011, **56**, 3703-3710.
69 J. S. Torrecilla, T. Rafione, J. García and F. Rodríguez, *J. Chem. Eng. Data*, 2008, **53**, 923-928.
70 J. Tong, M. Hong, Y. Chen, H. Wang, W. Guan and J.-Z. Yang, *J. Chem. Thermodyn.*, 2012, **54**, 352-357.
71 J.-y. Wang, X.-j. Zhang, Y.-q. Hu, G.-d. Qi and L.-y. Liang, *J. Chem. Thermodyn.*, 2012, **45**, 43-47.
72 U. Domańska, A. Pobudkowska and M. Rogalski, *J. Colloid Interf. Sci.*, 2008, **322**, 342-350.
73 H. F. D. Almeida, J. A. Lopes-da-Silva, M. G. Freire and J. A. P. Coutinho, *J. Chem. Thermodyn.*, 2013, **57**, 372-379.
74 J.-Y. Wang, F.-Y. Zhao, Y.-M. Liu, X.-L. Wang and Y.-Q. Hu, *Fluid Phase Equilibr.*, 2011, **305**, 114-120.
75 A. Wandschneider, J. K. Lehmann and A. Heintz, *J. Chem. Eng. Data*, 2008, **53**, 596-599.
76 M. Geppert-Rybczyńska, J. K. Lehmann and A. Heintz, *J. Chem. Eng. Data*, 2011, **56**, 1443-1448.
77 M. Geppert-Rybczyńska, J. K. Lehmann, J. Safarov and A. Heintz, *J. Chem. Thermodyn.*, 2013, **62**, 104-110.
78 Y.-H. Yu, A. N. Soriano and M.-H. Li, *Thermochim. Acta*, 2009, **482**, 42-48.
79 D. Waliszewski and H. Piekarski, *J. Chem. Thermodyn.*, 2010, **42**, 189-192.
80 D. Waliszewski, *J. Chem. Thermodyn.*, 2008, **40**, 203-207.

81 R. Ge, C. Hardacre, P. Nancarrow and D. W. Rooney, *J. Chem. Eng. Data*, 2007, **52**, 1819-1823.
82 W. Chen, L. Qiu, S. Liang, X. Zheng and D. Tang, *Thermochim. Acta*, 2013, **560**, 1-6.